Performance Improvement of Direct Torque Controlled Interior Permanent Magnet Synchronous Motor Drive by Considering Magnetic Saturation

Behrooz Majidi*† Jafar Milimonfared* Kaveh Malekian*

*Amirkabir University of Technology (Tehran Polytechnic),
Center of Excellence in Power Systems, No. 424, Hafez Ave., Tehran 15914, Iran.

† Corresponding author: bmx@aut.ac.ir

***Abstract*—The influence of magnetic saturation on the maximum torque per ampere strategy in constant torque region and field weakening strategy in constant power region for a direct torque controlled interior permanent magnet synchronous motor drive are discussed in this paper. In other words, by considering magnetic saturation, all optimal strategies and motor-inverter limitations are derived in the $T-|\psi_s|$ plane to apply in the direct torque control method. These strategies that take magnetic saturation into account and determine the optimal torque and flux commands are derived and implemented in direct torque control method. Simulation results on a prototype interior permanent magnet motor are included to validate the usefulness of the work.**

***Index Terms*—Direct torque control, field weakening strategy, interior permanent magnet synchronous motor, magnetic saturation, maximum torque per ampere strategy.**

I. INTRODUCTION

RECENTLY, the Interior Permanent Magnet Synchronous Motor (IPMSM) is widely used in high performance applications due to some its advantageous such as high torque to current ratio, high power to current ratio, high efficiency, low noise, and robustness [1]-[3]. In high performance variable speed drive systems, the motor speed should closely follow specified reference trajectory regardless any load disturbances, parameter variations and any model uncertainties [4].

In addition, in some applications, wide-speed operation of electric drives is desired [5]-[8]. In other words, operation in both constant torque region and constant power region is needed. The optimal behavior of drive can be achieved by considering Maximum Torque per Ampere (MTPA) strategy below the base speed and Field Weakening (FW) strategy above the base speed. It should be noted that the MTPA and FW strategies must be modified in order to consider magnetic saturation. This paper focuses on optimal torque control of direct torque controlled interior permanent magnet synchronous machines capable of operating in both the constant torque and the constant power region.

In the Interior Permanent Magnet (IPM) motor, since the effective air-gap length on the d-axis is large and the relative magnetic permeability of the Permanent Magnet (PM) is close to unity, the variation of the corresponding magnetizing inductance, L_d , due to magnetic saturation, is minimal. On the contrary, the effective air-gap length on the q-axis is small, and, therefore, the saturation is significant [9], [10].

II. MOTOR DYNAMIC BY CONSIDERING MAGNETIC SATURATION

The mathematic model of IPMSM in the rotor reference frame can be obtained from synchronous machine model. Due to constant field produced by permanent magnets, the field variation is zero. In this paper it is assumed that:

- Magnetic saturation is considerable;
- Core losses are negligible;
- The induced EMF is sinusoidal; and
- There is no dampener winding on rotor.

Using these assumptions, the voltages and torque equations could be written as,

$$\begin{pmatrix} V_q \\ V_d \end{pmatrix} = \begin{pmatrix} R & \omega_{re} L_d \\ -\omega_{re} L_q & R \end{pmatrix} \begin{pmatrix} i_q \\ i_d \end{pmatrix} + \begin{pmatrix} i_q & 0 \\ 0 & i_q \end{pmatrix} \begin{pmatrix} pL_q \\ pL_d \end{pmatrix} + \begin{pmatrix} L_q & 0 \\ 0 & L_d \end{pmatrix} \begin{pmatrix} pi_q \\ pi_d \end{pmatrix} + \begin{pmatrix} \omega_{re} \psi_f \\ 0 \end{pmatrix} \tag{1}$$

$$T_e = \frac{3P\psi_s}{4L_d L_q} [2\psi_f L_q \sin\delta - \psi_s (L_q - L_d) \sin 2\delta] \tag{2}$$

$$T_e = T_L + B\omega_{rm} + Jp\omega_{rm} \tag{3}$$

$$\omega_{rm} = \frac{1}{P} \omega_{re} \tag{4}$$

where, V_q, V_d are the q- and d-axis voltages; L_q, L_d are the q- and d-axis inductances; i_q, i_d are the q- and d-axis currents; R is the stator resistance per phase; ψ_f is the constant flux linkage due to rotor permanent magnet; ψ_s is the stator flux

978-1-4244-1742-1/08/$25.00 ©

linkage; δ is the load angle; ω_{rm}, ω_{re} are the mechanical and electrical rotor angular speed, respectively; P is the number of pair poles; p is the differential operator; T_e is the electro-magnetic torque; T_L is the load torque; B is the viscous coefficient; and J is the inertia constant.

III. Magnetic Saturation in IPMSM

In IPM synchronous motor, the magnetic saturation on the high-inductance axis (q-axis) is significant. The L_q inductance varies depending on the q-axis component of the magnetizing current i_{mq}, which is identical to i_q current, and can be represented by [10]-[12],

$$L_q = L_q(i_q) \tag{5}$$

where $L_q(i_q)$ is a nonlinear function of the i_q current that models the saturation effects. An acceptable approximation is that, two inductances are defined for the q-axis: an unsaturated inductance which applies for i_q current lower than i_{qs}, and a saturated one (linearly varied with the i_q current) for higher i_q current [13], [14].

$$L_q = \begin{cases} L_{qo}, & i_q < i_{qs} \\ L_{qo} - \beta(i_q - i_{qs}), & i_q > i_{qs} \end{cases} \tag{6}$$

where β is a coefficient expressing the saturation effect. Unlike the L_q inductance, the variation of L_d according to i_d is negligible and, therefore, L_d can be considered constant. Furthermore, mutual coupling effects between q- and d-axis could be assumed negligible [10].

The variation of L_q with respect to i_q, considered in a three phase IPM motor as illustrated in Fig. 1. The parameters of the IPM motor are given in Table I.

IV. Direct Torque Control Principle by Considering Magnetic Saturation

Fig. 2 shows the block diagram of a DTC-based ac motor drive. As shown in this figure, a switching table is used for inverter control such that the torque and flux errors are kept within the specified bands.

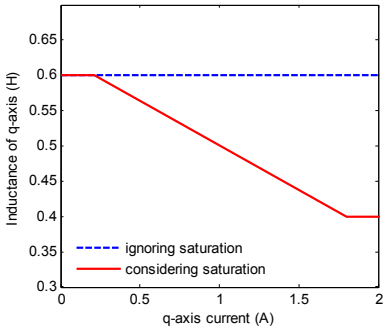

Fig. 1. The variation of q–axis inductance (L_q) with respect to the q–axis current (i_q).

TABLE I
Motor Parameters

Rated voltage	240 V
Rated frequency	60 Hz
Number of pair poles	2
d-axis inductance	0.375 H
q-axis inductance	$\begin{cases} 0.601, H & i_q < (0.21A) \\ 0.601 - 0.1258(i_q - 0.21), H & i_q > (0.21A) \end{cases}$
Stator resistance	19.4 Ω
Magnetic flux constant	0.447 v/rad/s
Rotor inertia	0.8×10^{-3} kgm^2

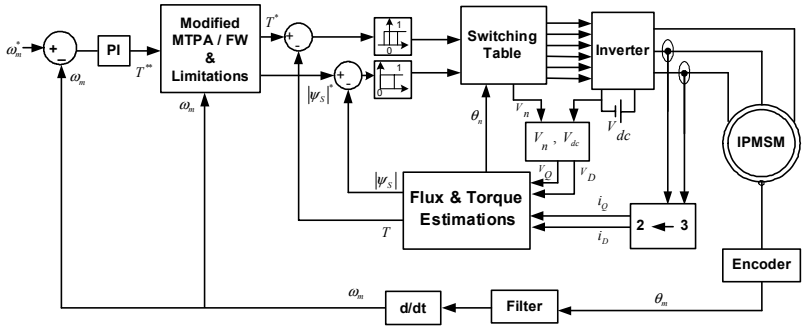

Fig. 2. Block diagram of the proposed direct torque controlled IPMSM drive.

Compared to the conventional current vector control method, the DTC scheme has the following features.

- There are no current control loops, hence, the current is not regulated directly;
- Coordinate transformation is not required;
- There is no separate voltage pulsewidth modulator; and
- Stator flux vector and torque estimation is required.

In the current vector control method, since q- and d-axis current components are directly controlled, all control strategies and motor-inverter limitations are considered in the $i_q - i_d$ plane. Unlike current vector control, torque and stator flux are directly controlled in the direct torque control method. As a result, all control strategies and limitations in the $i_q - i_d$ plane must be transmitted into the $T - |\psi_s|$ plane. Because each point in the $i_q - i_d$ plane can be transmitted into its corresponding point in the $T - |\psi_s|$ plane using (7) and (8), all control strategies and limitations can be mapped into the $T - |\psi_s|$ plane point by point.

$$T = \frac{3}{2} P \left[\psi_f + \left(L_d - L_q(i_q) \right) i_d \right] i_q \qquad (7)$$

$$|\psi_s| = \sqrt{(L_d i_d + \psi_f)^2 + \left(L_q(i_q) i_q \right)^2} \qquad (8)$$

It should be noted that saturation of the q-axis inductance should be considered in (7) and (8) to achieve correct mapping. In the following sections, the current and voltage constraints as well as the optimal strategies in the constant torque and constant power regions are explained.

A. Constraints

Considering the voltage and current constraints, the armature voltages and currents could be written as,

$$I_a = \sqrt{i_d^2 + i_q^2} \le I_{am} \qquad (9)$$

$$V_a = \sqrt{v_d^2 + v_q^2} \le V_{am} \qquad (10)$$

where I_{am} is continuous armature current rating in continuous operation or maximum available current of the inverter. The maximum voltage V_{am} is the maximum available output voltage of the inverter. The critical condition of (9) (i.e., $I_a = I_{am}$) is given by the current limit circle in the $i_q - i_d$ plane, which is independent with respect to the magnetic saturation, as shown in Fig. 3(a). For each (i_q, i_d) pair satisfying (9), torque and $|\psi_s|$ can be found and plotted in the $T - |\psi_s|$ plane. Figs. 3(b)-(c) indicate the current limit trajectory by ignoring and considering saturation while mapping, respectively.

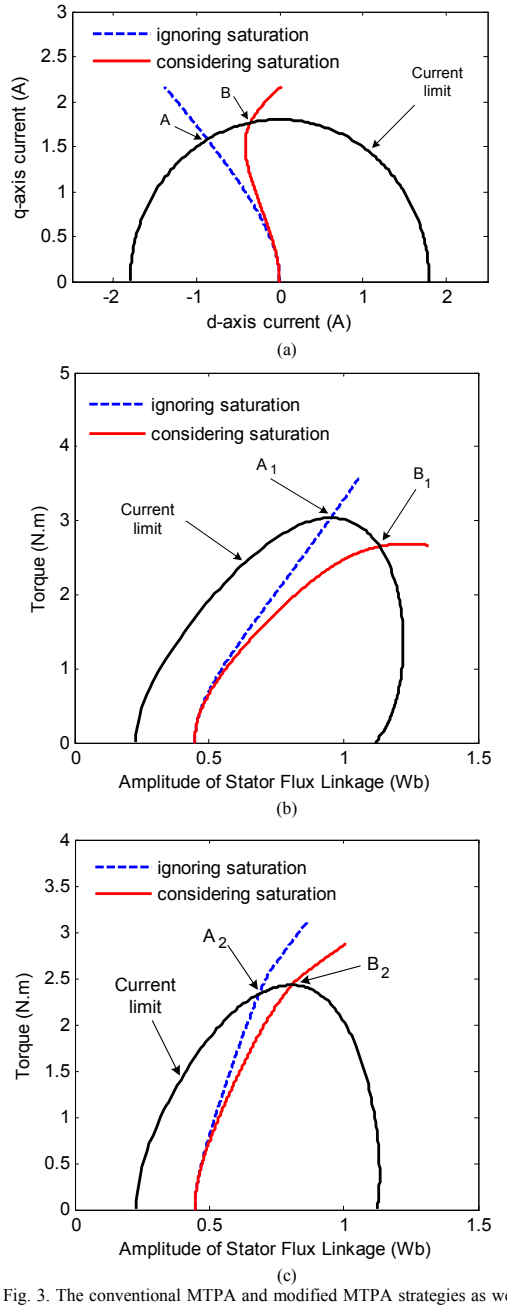

Fig. 3. The conventional MTPA and modified MTPA strategies as well as the current limit: (a) in the $i_q - i_d$ plane; (b) mapped into the $T - |\psi_s|$ plane by ignoring saturation while mapping; and (c) mapped into the $T - |\psi_s|$ plane by considering saturation while mapping.

B. Control in Constant Torque Region

The most popular strategy in the constant torque region is maximum torque per ampere. The MTPA strategy must be modified in order to consider magnetic saturation. The relationships between i_q and i_d which satisfy MTPA by ignoring and considering saturation are given by (10) and (11), respectively [8], [15].

$$i_d = \frac{\psi_f}{2(L_q - L_d)} - \sqrt{\frac{\psi_f^2}{4(L_q - L_d)^2} + i_q^2} \tag{10}$$

$$i_d = \frac{\psi_f - \sqrt{\psi_f^2 + 4i_q^2(L_q - L_d)\left[(L_q - L_d) - (L_q')i_q\right]}}{2\left[(L_q - L_d) - (L_q')i_q\right]} \tag{11}$$

Considering (6), L_q' could be written as

$$L_q' = \begin{cases} 0 & i_q < i_{qs} \\ -\beta & i_q > i_{qs} \end{cases} \tag{12}$$

Fig. 3(a) illustrates the MTPA trajectories by considering saturation and ignoring saturation in the $i_q - i_d$ plane. Figs. 3(b)-(c) show both conventional and modified MTPA trajectories mapped into the $T - |\psi_s|$ plane by ignoring and considering saturation while mapping, respectively.

The command vector producing maximum torque, $T_{\max}$, is the cross point of the MTPA trajectory and the current-limit, which corresponds to points A and B for traditional MTPA and modified MTPA strategies, respectively, in all Figs. 3(a)-(c). The maximum torque corresponding to the conventional MTPA strategy mapped by ignoring saturation (corresponding to point A_1) can not be produced because a real IPMSM magnetically saturates, however, it is greater than the maximum torque corresponding to the modified MTPA mapped by considering saturation (corresponding to point B_2). In other words, by considering effect of saturation on both derivation of MTPA relationship and map of this relationship, the maximum possible torque can be achieved.

C. Control in Field Weakening Region

The torque capability in field weakening region is determined by both of the voltage and the current limits. In the steady state, the voltage constraint could be expressed as

$$V_o = \sqrt{v_{do}^2 + v_{qo}^2} \le V_{om} \tag{13}$$

where,

$$v_{do} = -\omega_{re} L_q(i_q) i_q,\ v_{qo} = \omega_{re} L_d i_d + \omega_{re}\psi_f \tag{14}$$

$$V_{om} = V_{am} - RI_{am} \tag{15}$$

The "o" subscripts are defined to simplify the control algorithm. Fig. 4 illustrates voltage limits in both considering saturation and ignoring saturation in $i_q - i_d$ plane. Figs. 4(b)-(c) show both conventional and modified voltage limit trajectories mapped into the $T - |\psi_s|$ plane by ignoring and considering saturation while mapping, respectively.

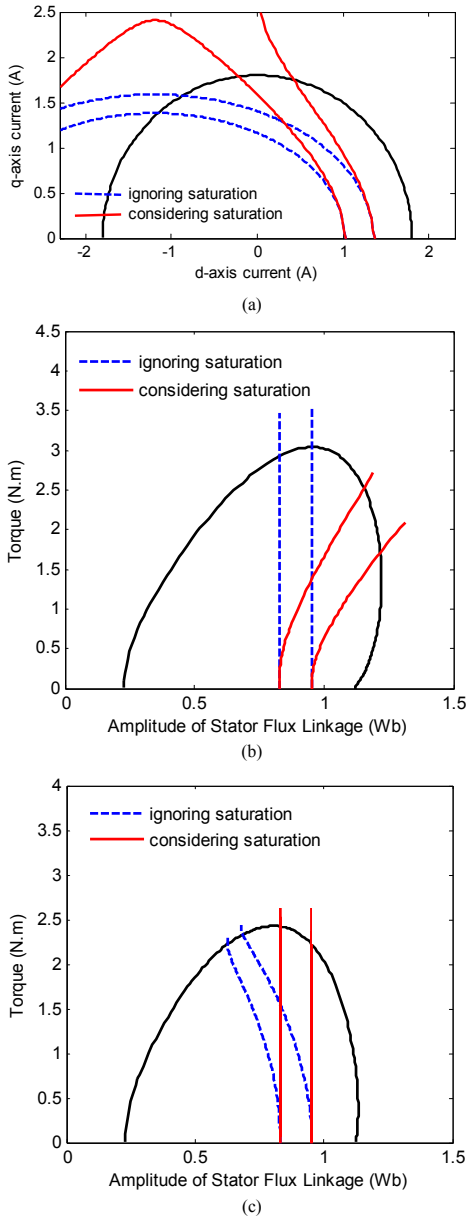

Fig. 4. The conventional and modified voltage limits as well as the current limit: (a) in the $i_q - i_d$ plane; (b) mapped into the $T - |\psi_s|$ plane by ignoring saturation while mapping; and (c) mapped into the $T - |\psi_s|$ plane by considering saturation while mapping.

As shown in Fig. 4(c), the modified voltage limits mapped by considering saturation are vertical lines in the $T-|\psi_s|$ plane. Also, a given relationship in the $T-|\psi_s|$ plane can be derived for the voltage limit, which verifies the modified voltage limit trajectories in Fig. 4(c).

Combining (13) and (14) yields,

$$\left(-L_q(i_q)i_q\right)^2+\left(L_d i_d+\psi_f\right)^2=\left(\frac{V_{om}}{\omega_{re}}\right)^2 \tag{16}$$

So

$$|\psi_s|=\frac{V_{om}}{\omega_{re}} \tag{17}$$

This equation is independent with respect to the magnetic saturation. As a result, the modified voltage limit are, always, vertical lines in the $T-|\psi_s|$ plane, regardless of motor saturates or how variation of L_q with respect to i_q is.

When the rotor speed is below the base speed, the voltage limit line is on the right side of the intersection of the MTPA and current limit trajectories (point B_2) and, therefore, the voltage limit is always satisfied with MTPA trajectory control. When the rotor speed is increased above the base speed, voltage limit line moves to left and the stator flux linkage should be reduced according to (17) for FW operation. In other words, for operation above the base speed, the amplitude of the stator flux linkage is approximately inversely proportional to the rotor speed.

V. Simulation Results

The complete proposed IPMSM drive, as shown in Fig. 2, has been simulated using Matlab/Simuink for the prototype IPMSM of Table I.

The direct torque controlled IPMSM drive incorporating traditional MTPA and FW strategies has been also simulated in order to compare the performance to those obtained from the proposed drive system. In order to make a fair comparison, the same limitations are considered for both of them. Also, several tests have been performed to evaluate the performance of the proposed IPMSM drive system.

The simulated responses are shown in Figs. 5 (a)-(b) for both of the conventional and modified direct toque controlled drive systems, to see the starting performance as well as the response with a step change in the command speed. The drive system is started with the speed reference set at 400 rpm. It is seen from Fig. 5(a) that the proposed drive can follow the command speed within 0.1 Sec., whereas the conventional direct toque controlled drive follow the command speed within 0.12 Sec. because, as shown in Fig. 5(b), the maximum available torque is less in the conventional system. At $t=0.3$ Sec., command speed changed into 800 rpm. In this case, the modified system has better performance as well.

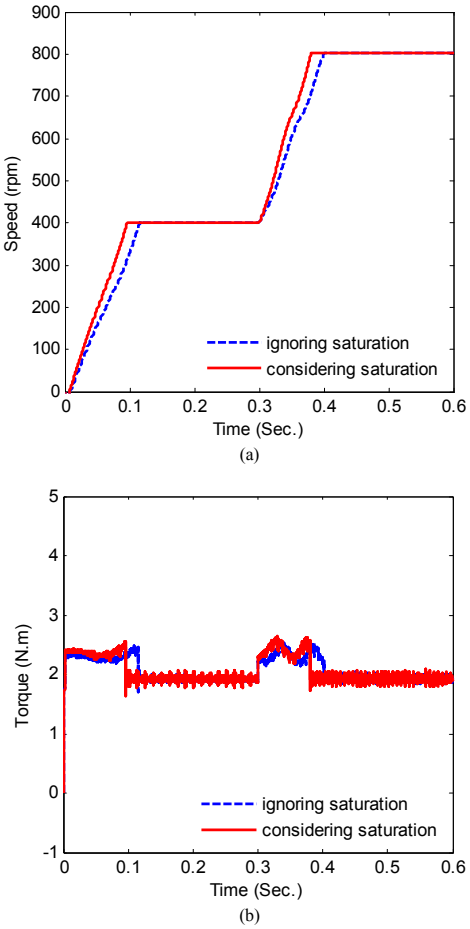

Fig. 5. Simulated responses of the both conventional and modified drive systems: (a) speed responses and (b) torque responses.

In another simulation test, the proposed drive performance including speed, torque are observed under different operating conditions such as sudden change in load and step change in command speed over wide speed range. The proposed drive system is started at no load condition with the rotor speed of 800 rpm. At $t=0.1$ Sec., a step change in load torque (1.1 N.m) is applied to the motor shaft, and at $t=0.2$ Sec., the command speed changes into 2000 rpm (above the base speed). The proposed drive responses are shown in Fig. 6(a)-(b). It is shown that both drive systems are also capable of following the command speed above the base speed, but dynamic of responses for the modified drive system is better than ones obtained for the conventional system.

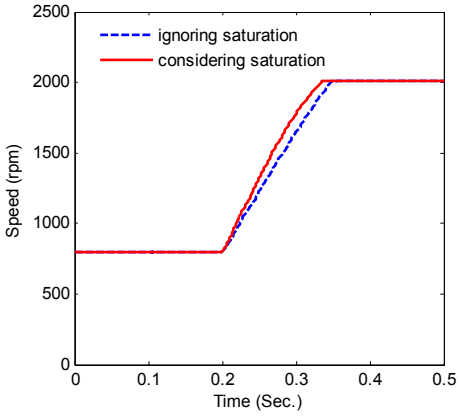

(a)

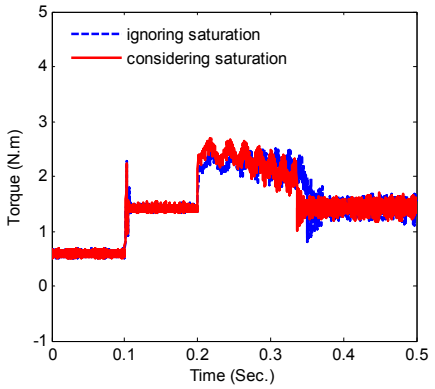

(b)

Fig. 6. Simulated responses of the both conventional and modified drive systems with respect to sudden change in load and step change in speed command above the base speed: (a) speed responses and (b) torque responses.

VI. CONCLUSION

Considering magnetic saturation, the modified MTPA and FW strategies as well as drive limitations have been derived in the $T-|\psi_s|$ plane to apply in the direct torque control method. The proposed direct torque controlled IPMSM drive has been simulated for an IPM motor. The validity of the proposed IPMSM drive has been established in simulation at different operating conditions by considering saturation. In order to prove the superiority of the proposed controller, a performance comparison with the conventional direct torque controlled IPMSM drive has also been provided. The simulation results show ability of the proposed technique at different operation condition such as sudden load change and step change of speed (over wide speed range).

REFERENCES

[1] G.R. Slemon, *Electric Machines and drives*, Addison-Wesley Publication Company, 1992, pp. 503-511.

[2] J. K. Gieras and M.Wing, *Permanent Magnet Motor Technology: Design and Applications*, New York: Marcel-Dekker, 1997.

[3] P. Vas, *Sensorless Vector and Direct Torque Control*, Oxford, 1998, pp. 87-90.

[4] K. Malekian and J. Monfared, "A Genetic Based Fuzzy Logic Controller for IPMSM Drive over Wide Speed Range," *Electric Machines & Drives Conference, IEMDC '07, IEEE International*, vol. 1, pp. 847–853, 3-5 May 2007.

[5] T. M. Jahns, "Flux- weakening Regime Operation of an Interior Permanent-magnet Synchronous motor Drive," *IEEE Trans. Ind. Appl.,* vol. IA-23, no.4, pp.681~689, 1986.

[6] B. K. Bose, "A High-Performance Inverter-Fed Drive System of an Interior Permanent Magnet Synchronous Machine", *IEEE Trans. Ind. Appl.,* vol. IA-24, no.6, pp.987~997, 1988.

[7] S.R. MacMinn and T. m. Jahns, "Control Techniques for Improved High-Speed Performance of Interior PM Synchronous Motor Drive*," IEEE Trans. Ind. Appl.*, vol. IA-27, no.4, pp.997~1004, 1991.

[8] S.Morimoto, M Sanada and Y. Taketa, "Wide-Speed Operation of Interior Permanent Magnet Synchronous Motor with High-Performance Current Regulator," *IEEE Trans. Appl.*, vol. IA-30. no.4, pp.920-926, 1994.

[9] S. A. Nasar, I. Boldea, and L. E. Unnewehr, *Permanent Magnet, Reluctance, and Self-Synchronous Motors. Florida*: CRC Press, Inc., 1993.

[10] B. J. Chalmers, S. A. Hamed, and G. D. Baines, "Parameters and performance of a high-field permanent-magnet synchronous motor for variable-frequency operation," *IEE Proc.*, pt. B., vol. 132, no. 3, pp.117–124, May 1985.

[11] N. Bianchi and S. Bolognani, "Parameters and volt–ampere rating of a synchronous motor drive for flux-weakening applications," *IEEE Trans. Power Electronics*, vol. 12, no. 5, pp. 895–903, Sept. 1997.

[12] S. Morimoto, Y. Takeda, T. Hirasa, and K. Taniguchi, "Expansion of operating limits for permanent magnet motor by current vector control considering inverter capacity," *IEEE Trans. Ind. Appl.*, vol. 26, no. 5, pp. 866–871, Sept./Oct. 1990.

[13] B. J. Chalmers, "Influence of saturation in brushless permanent-magnet motor drives," *IEE Proc*., pt. B, vol. 139, no. 1, pp. 51–52, Jan. 1992.

[14] B. J. Chalmers, R. Akmese, and L. Musaba, "Validation of procedure for prediction of field-weakening performance of brushless synchronous machines," *in Proc. ICEM 1998*, vol. 1, Istanbul, Turkey, pp. 320–323.

[15] C. Mademlis and V. G. Agelidis, "On Considering Magnetic Saturation with Maximum Torque to Current Control in Interior Permanent Magnet Synchronous Motor Drives," *IEEE Trans. on Energy Conversion,* vol. 16, no. 3, Sep. 2001.